# Strong Carrier-Phonon Coupling in Lead Halide Perovskite Nanocrystals

# Supporting Information

Claudiu M. Iaru,[*,†] Jaco J. Geuchies,[‡] Paul M. Koenraad,[†] Daniël Vanmaekelbergh,[‡] and Andrei Yu. Silov[*,†]

†*Applied Physics department, Eindhoven University of Technology, P.O. Box 513, 5600 MB, Eindhoven, The Netherlands*

‡*Condensed Matter and Interfaces, Debye Institute for Nanomaterials Science, Utrecht University, Princetonplein 1, 3508 TA, Utrecht, the Netherlands*

E-mail: C.M.Iaru@tue.nl; A.Y.Silov@tue.nl

## Room Temperature PL and TEM analysis of nanocrystals

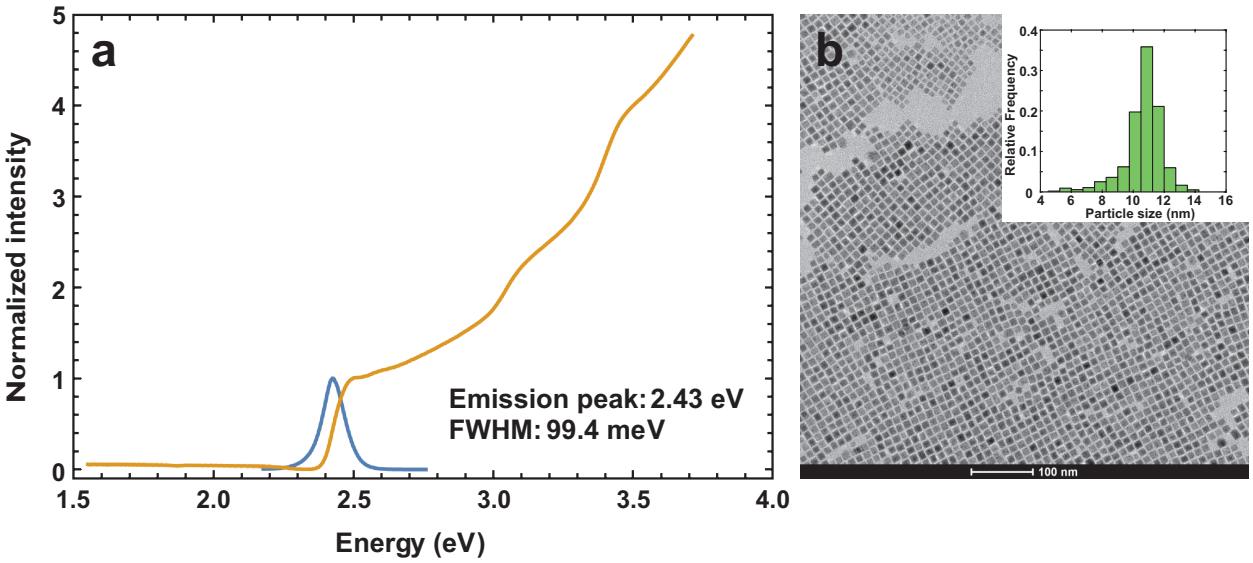


Figure 1: a) Absorption and PL spectrum obtained from the colloidal $CsPbBr_3$ NC solution at room temperature. b) TEM image of the $CsPbBr_3$ nanocrystals investigated in a). The inset shows the particle size distribution, with a mean of 10.6 ± 1.3 nm

## Temperature dependence of FWHM

The dependece of the overall FWHM on sample temperature is shown in figure 2, for two different nanocrystal samples, under non-resonant excitation conditions. In the quasi-resonant case, a blue shift of the spectrum with increasing temperature led to significant overlap with the laser line, making the correct determination of the FWHM impossible. The data has been fitted using the following equation:

$$FWHM(T) = \frac{A}{\exp\frac{E_{ph}}{k_B T} - 1} + C, \tag{1}$$

which contains the LO phonon contribution, given by the Bose-Einstein distribution, where $E_{ph}$ is the LO phonon energy and the proportional term, $A$, denotes the coupling strength. The inhomogeneous broadening term $C$ is unrelated to thermal effects, and represents the

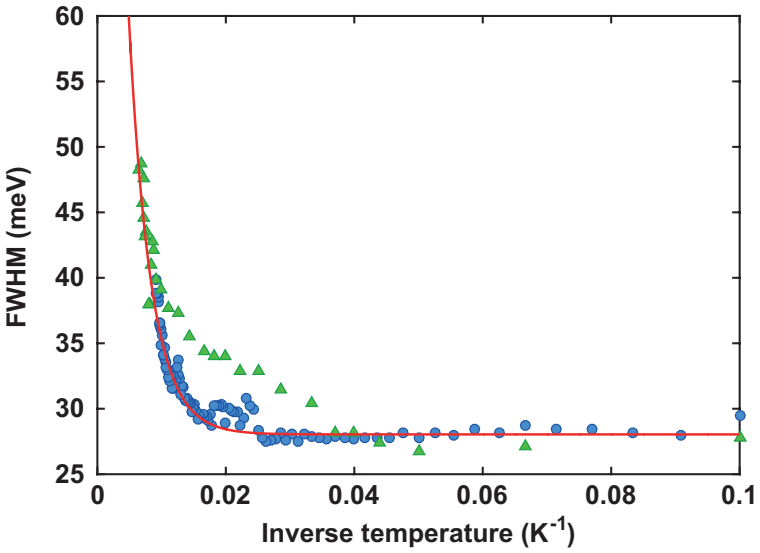


Figure 2: Temperature dependence of the overall FWHM of the PL spectrum, for non-resonant excitation. The red line is a fit corresponding to the phonon broadening equation used by Sebastian *et al*[1] and Wright *et al.*[2] The green and blue markers represent data from measurements corresponding to two different nanocrystal samples.

FWHM at low temperatures, where no significant thermal broadening occurs.[1,2] The fit shows that LO phonon coupling can correctly explain the observed broadening behavior. Low temperature spectra show little to no temperature dependence up to 30-40 K, suggesting only negligible acoustic broadening, whereas at high temperatures, above 100 K, LO phonon coupling takes over as the phonon occupation number increases. We obtain a low temperature FWHM of 28 meV, which is consistent with results from other nanocrystal samples. The LO phonon energy of 25 meV is within the FWHM of the 165 $cm^{-1}$ mode reported by Stoumpos *et al.* The slightly higher energy is probably related to the colloidal synthesis, as different nanocrystal batches show rather different spectral shapes, due to varying $S$ parameter values. Moreover, in equation 1 we neglect the linear broadening term related to acoustic phonons, such that the LO phonon energy is most likely lower than 25 meV. We observe an increase in FWHM in the vicinity of 50 K which is probably related to a form of carrier trapping, similarly reported by Wright *et al*, for methyl-ammonium-based perovskites,[2] and it has been excluded from the fitted data. Extrapolation of the fit up to room temperature leads to a FWHM value on the order of 78 meV, which is similar to our measurement in figure 1. The

additional broadening in figure 1 can be explained as a consequence of the measurement being performed in solution, with a broad area of excitation, as opposed to a confocal measurement on a drop-casted sample in figure 2.

## Processing of Acquired PL Data Using Matlab

The acquired PL data was smoothed out using a median filter (Matlab command `medfilt1()`). The effect is shown in Figure 3. In order to fit the filtered data points, a triple Voigt function was defined, using as parameters the height of each peak (`i1,i2,i3`), the position of the zero phonon line (`x0`), the FWHM of the Gaussian (`sigma`) and Lorentzian (`gamma`) components of the profile, and the fixed spacing between the bands, representing the LO phonon energy (`hw`). We define `x` as an independent variable, over the range of interest, and use the Faddeeva function, `W()` (defined elsewhere), in the definition of each Voigt profile. The fitting function is defined as follows:

```
F=fittype('i1 * real(W((x-x0+1i*gamma/2) / (sigma/2.35482*sqrt(2)))) / (
    sigma/2.35482*sqrt(2*pi)) + i2 * real(W((x -x0+hw+1i*gamma/2) / (sigma
    /2.35482*sqrt(2)))) / (sigma/2.35482*sqrt(2*pi)) + i3 * real(W((x-x0+2*
    hw+1i*gamma/2) / (sigma/2.35482*sqrt(2)))) / (sigma/2.35482*sqrt(2*pi))
    ', 'independent', {'x'}, 'coefficients', {'i1','i2','i3','gamma','hw','
    x0','sigma'})
```

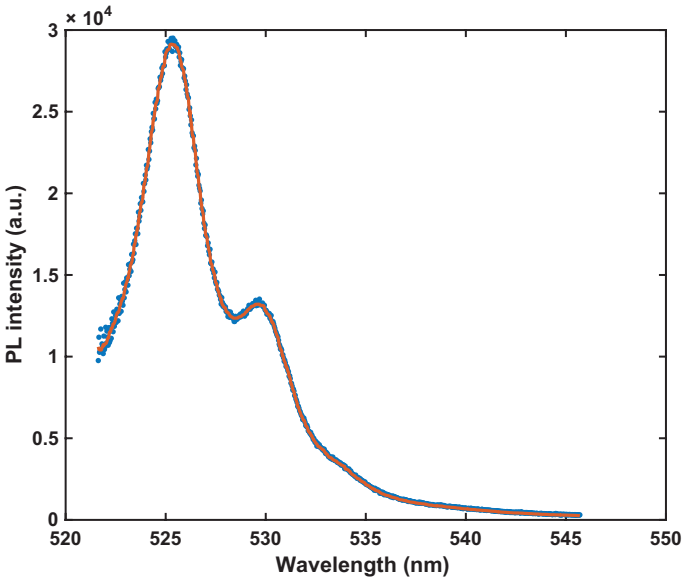


Figure 3: An example of raw and filtered PL line data for a quasi-resonant measurement. The median filter is used to reduce noise, after which the fitting procedure is applied to the filtered data.

## Gauss and Lorentz components of fitted Voigt profiles

The fitted Voigt profiles represent a convolution between a Lorentzian and Gaussian profile, and the FWHM of both the Lorentzian and Gaussian components constitute parameters for the fit function used in our calculations. As such, we may acquire additional information with regards to broadening, by investigating the differences in Lorentzian and Gaussian components between non-resonantly and quasi-resonantly excited samples. In order to illustrate the increased occupation of localized states under quasi-resonant excitation, figure 4 shows the distribution of lorentizan and Gaussian FWHM. The Lorentzian component is linked to homogeneous broadening, whereas the Gaussian component is indicative of inhomogeneous broadening, which reflects local differences in energy, such as those due to carrier localization in an inhomogeneous charge distribution and electric field. Accordingly, we observe a similar distribution of Lorentzian FWHM under both excitation schemes, indicating that additional broadening in the non-resonant case must result from inhomogeneous mechanisms. Under non-resonant excitation the Gaussian components reveal a relatively uniform probability

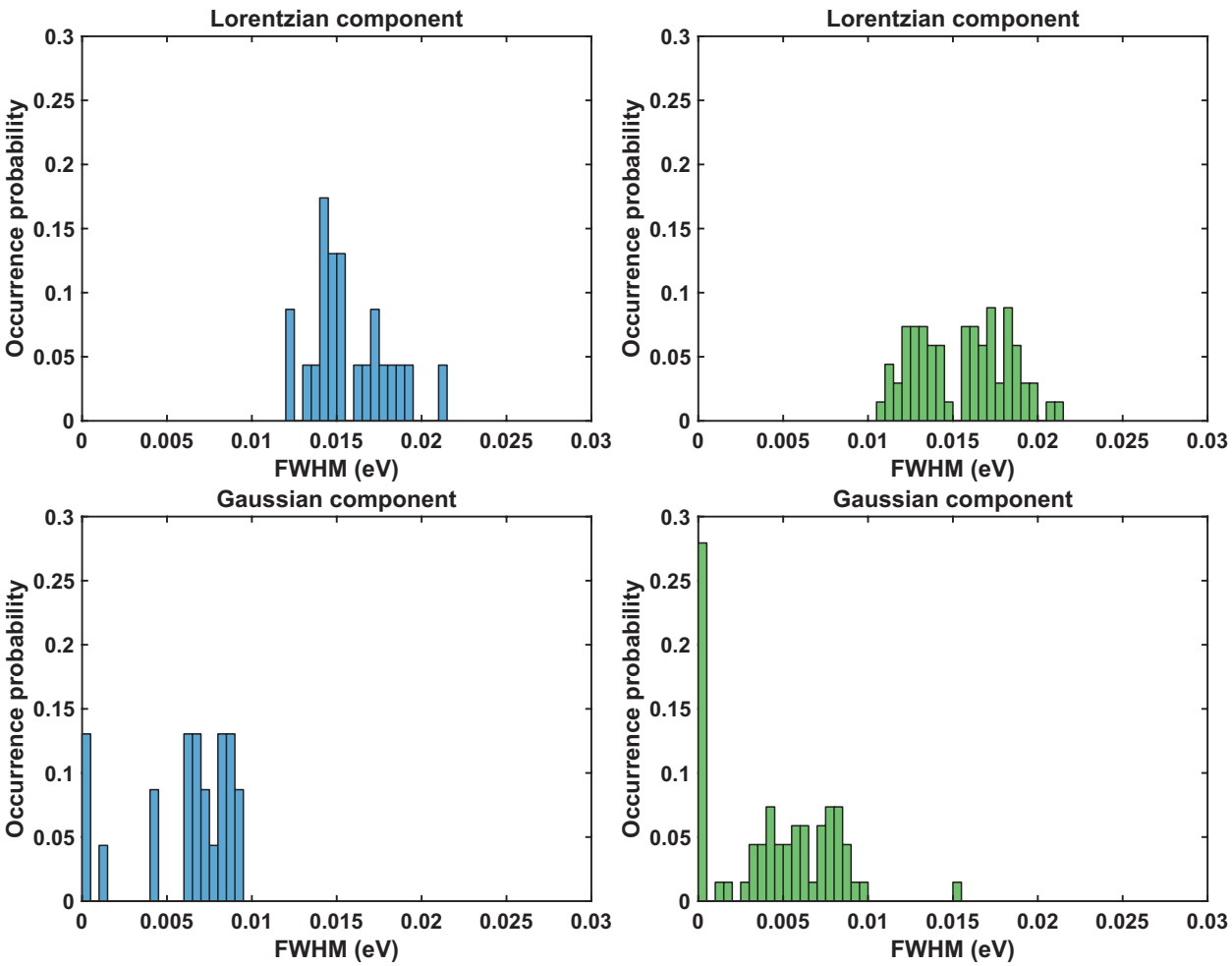


Figure 4: FWHM of the Lorentzian (a, b) and Gaussian (c, d) components which form the Voigt profiles fitted to the measurement data. The values of FWHM are fitting parameters for the function described in the previous section.

distribution, such that both inhomogeneously broadened and unbroadened PL bands are equally likely, as carriers must thermalize before photon emission. In contrast to this, the distribution under quasi-resonant excitation shows a significant increase in the number of Gaussian FWHM with a value of zero. This is most likely a consequence of the excitation scheme, in which the higher energy (delocalized) states are resonantly excited, subsequently transferring into localized states by emitting a single LO phonon. As the initial energy state is the same for all resonantly excited carriers, the emission of an LO phonon results in the transfer into a similarly well-defined state. In these situations, Gaussian broadening is not significant, as the recombination energy is directly linked to the well-defined energy

of the exciting photon. The non-zero Gaussian FWHM values obtained under the same quasi-resonant excitation scheme reflect the spatial inhomogeneity of the localized state distribution. If carriers cannot resonantly de-excite into a localized state by emitting a single LO phonon, the situation becomes similar to non-resonant excitation, and a wide distribution of non-zero Gaussian FWHM is observed.

Figure 5 shows the distribution of Voigt FWHM for both excitation conditions. The FWHM of the Voigt profiles were calculated from the Lorentzian and Gaussian FWHM, using the following empirical formula:[3]

$$FWHM = 0.5346 \cdot \gamma + \sqrt{0.2166 \cdot \gamma^2 + \sigma^2}, \tag{2}$$

where $\gamma$ is the FWHM of the Lorentzian component, and $\sigma$ is that of the Gaussian component. We observe a reduction in the mean FWHM in the quasi-resonant case, which is directly correlated to the absence of inhomgeneous broadening in a larger number of measurements, and a lower overall mean value, compared to the case of non-resonant excitation.

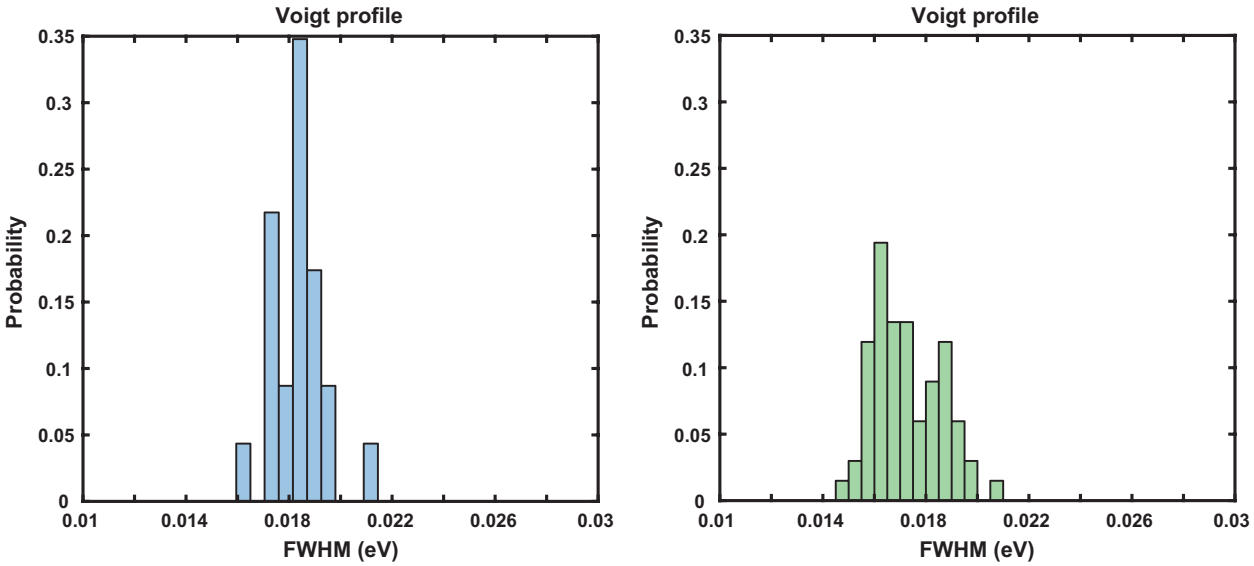


Figure 5: Voigt profile FWHM for non-resonant (blue) and quasi-resonant (green) excitation. The FWHM were calculated using equation 2

# References


1. Sebastian, M.; Peters, J. A.; Stoumpos, C. C.; Im, J.; Kostina, S. S.; Liu, Z.; Kanatzidis, M. G.; Freeman, A. J.; Wessels, B. W. Excitonic Emissions and Above-Band-Gap Luminescence in the Single-Crystal Perovskite Semiconductors $CsPbBr_3$ and $CsPbCl_3$. *Phys. Rev. B* **2015**, *92*, 235210.

2. Wright, A. D.; Verdi, C.; Milot, R. L.; Eperon, G. E.; Pérez-Osorio, M. A.; Snaith, H. J.; Giustino, F.; Johnston, M. B.; Herz, L. M. Electron-Phonon Coupling in Hybrid Lead Halide Perovskites. *Nat. Commun.* **2016**, 7:11755, doi: 10.1038/ncomms11755.

3. Olivero, J. J.; Longbothum, R. L. Empirical Fits to the Voigt Line Width: A Brief Review. *J. Quant. Spectrosc. Radiat. Transfer* **1977**, *17*, 233–236.